Materials Physics and Mechanics 21 (2014) 1-7 Received: March 23, 2014

MOLECULAR DYNAMIC STUDY FOR ULTRATHIN NICKEL NANOWIRES AT THE SAME TEMPERATURE

M.D. Starostenkov[1], M.M. Aish[1,2*]

[1]I.I. Polzunov Altai State Technical University, Barnaul, Russia

[2]Physics Department, Faculty of Science, Menoufia University, Egypt

*e-mail: mohamedeash2@yahoo.com

Abstract. Molecular Dynamics (MD) simulations have been carried out on pure ultrathin Nickel (Ni) crystal with face-centered cubic (FCC) lattice upon application of uniaxial tension at nanolevel with a speed of 20 m/s. The deformation corresponds to the direction <001>. To the calculated block of crystal - free boundary conditions are applied in the directions <100>, <010>. Morse potential was employed to carry out three dimensional molecular dynamics simulations. A computer experiment is performed at a temperature corresponding to 10 K, 300 K and 1000 K. MD simulation used to investigate the effect of long of ultrathin Ni nanowire on the nature of deformation and fracture. The engineering stress–time diagrams obtained by the MD simulations of the tensile specimens of these ultrathin Ni nanowires show a rapid increase in stress up to a maximum followed by a gradual drop to zero when the specimen fails by ductile fracture. The feature of deformation energy can be divided into four regions: quasi-elastic, plastic, flow and failure. The results showed that breaking position depended on the nanowire length.

1. Introduction

There are a number of publications on mechanical properties of Ni nanowires in literature [1-6]. A three-dimensional nanowire with rectangular cross-section is simulated as in Fig. 1. The initial atomic configuration is positioned at the ideal lattice sites. The X, Y, and Z coordinate axes represent the lattice directions [100], [001], and [010], respectively. The estimated size of the crystal unit was for various experiments of 63 atoms (5 atoms along the edges at the bottom and 5 - in height) to 1375 atoms (150 atoms along the edges at the bottom and 5 - in height). The total sample consists of two parts. One part is designed as the active zone in which atoms move according to the inter-atomic potential; the other part is the boundary zone where positions of atoms are given by prescribed boundary conditions. The periodic boundary condition is applied in the length direction, i.e., the Z axis. The surfaces in the X and Y directions are free. The existence of those free surfaces will result in relaxation motion of the atoms near the surfaces, which then minimizes the total energy of the system.

In each simulation the temperature is kept constant by the direct velocity scaling method [7]. After full relaxation, extension strain loading is applied by uniformly scaling the Z coordinates. The atoms at each end are constrained, and can only displace in the Z direction during each loading step. The stepwise tensile strain is 0.02. It is relaxed for some time in each step. Both the strain step and relaxation time determine the strain rate. The tension/relaxation step is repeated until the model fails.

2. Model and simulation method

In this paper for calculating the dynamics of the atomic structure of the method of molecular

dynamics using paired Morse potential function [6-10], suitable in terms of their computing time and quality of results.

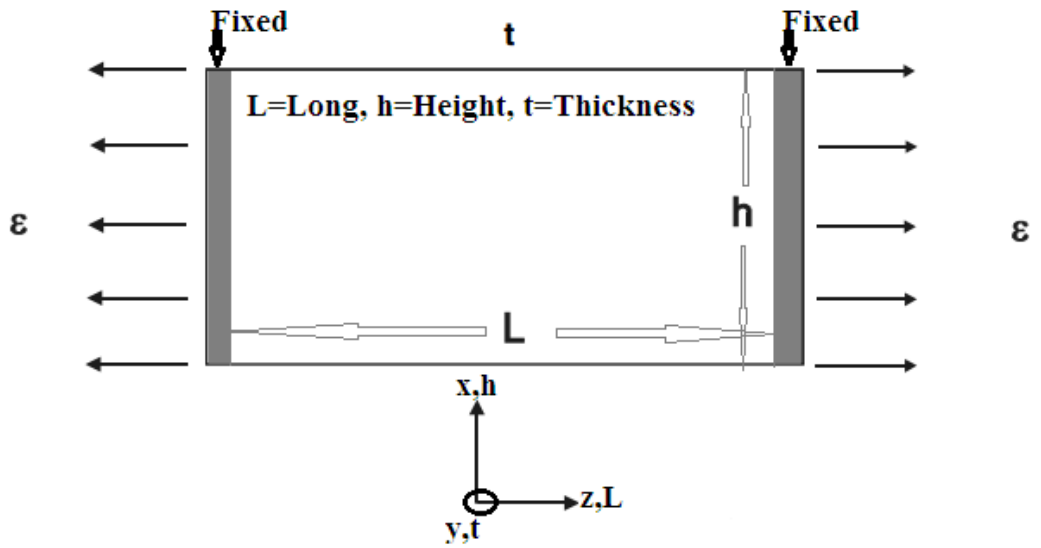

Fig. 1. Geometry of nanowire subjected to uniaxial tension under constant strain rate.

Morse pair potential is written as:

$$\varphi_{KL}(r) = D_{KL}\beta_{KL}e^{-\alpha_{KL}r}\left[\beta_{KL}e^{-\alpha_{KL}r} - 2\right],$$

where α_{KL}, β_{KL}, D_{KL} - parameters defining the interaction of pairs of atoms of type K and L; r - the distance between the atoms. The specific potential parameters are listed in [8, 11] when the potential is determined, the atomic force F is given as the derivative of the potential energy, namely

$$F = \frac{d\varphi_{KL}(r)}{dr}.$$

The object of investigation is taken ultrathin systems of Ni nanowires. Nanowire structure is presented in the form of a face-centered cubic cell. A computer experiment is performed at a temperature corresponding to 10 K, 300 K and 1000 K, at any stage of deformation involving the possibility of chilling calculation unit for detailed analysis of the structural changes occurring in it [6, 12, 13].

3. Atom Snapshot during Tensile Deformation

To visualize the tensile deformation process of the Ni nanowire at the temperature of 300 K, snapshots of atomic rearrangements are shown in Figs. 2, 3. After relaxation, the surface atoms move a little and the whole configuration maintains regularity when there is no strain load, as displayed in Figs. 2a, 3a. When the model stretches in the height direction, necking appears near the middle of the model and then becomes increasingly distinct, and the deformation concentrates in the neck region as shown in Figs. 2b and 2c. In the end, the plastic deformation causes ductile shear fracture as shown in Figs. 2d, 3c. This deformation evolution is also different from that of Ni bulk, in which there is no necking and brittle fracture occurs suddenly near the middle of the model [11]. From Figs. 2 and 3 the tensile mechanism of the atomistic simulations at the nanometer dimension shows results that agree with the mechanism of plasticity observed in macroscale experiments.

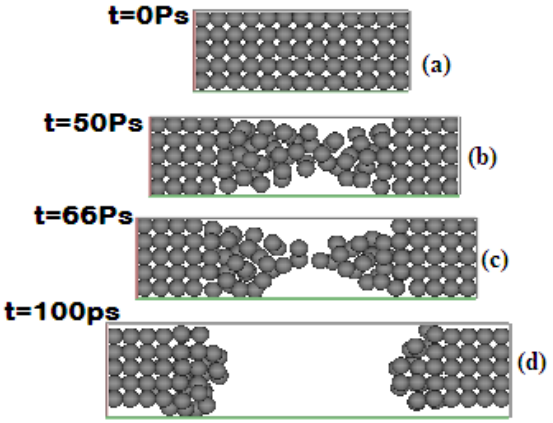

Fig. 2. Snapshots of the atomic configuration rearrangement of a 5x5x5 Ni nanowire at the temperature of 300 K. The configurations presented correspond to the following times: (a) 0 ps, (b) 50 ps, (c) 66 ps, and (d) 100 ps.

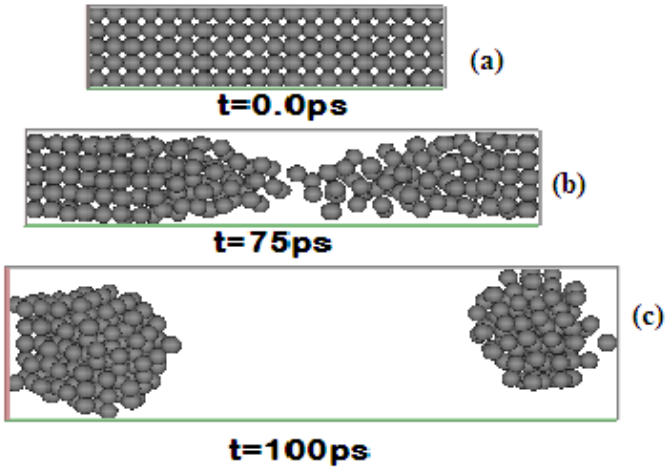

Fig. 3. Snapshots of the atomic configuration rearrangement of a 5x5x20 Ni nanowire at the temperature of 300 K. The configurations presented correspond to the following times: (a) 0 ps, (b) 75 ps, and (c) 100 ps.

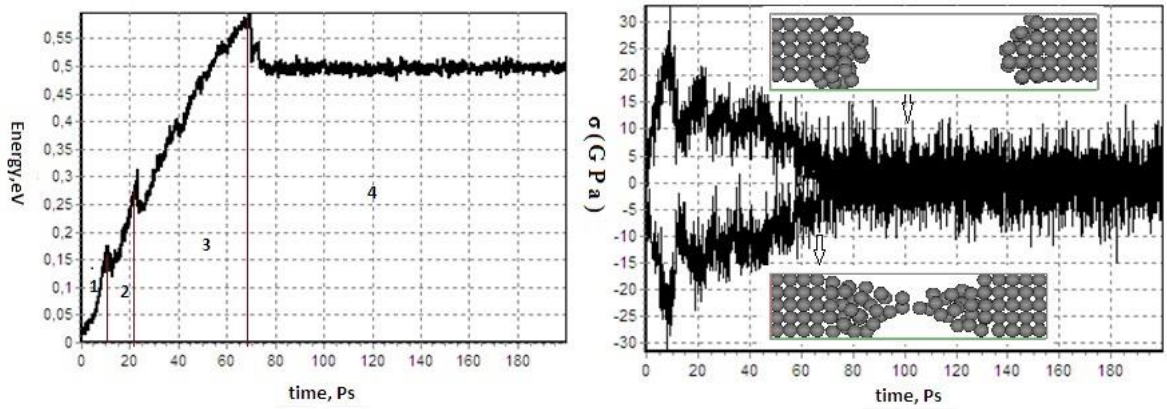

Fig. 4. The dependence of the stored energy of deformation of the experiment at 300 K for nickel-5x5x5 (a)
and the relation of stress with time at temperatures 300 K for nickel-5x5x5 (b).

4. Effect of nanowire length and mechanical properties

To discuss the effect of nanowire length, a constant base of 5x5 nm was set and the length was varied in the range 5–150 nm in the simulations. In this work, MD simulations are performed for ultrathin Ni nanowire subject to uniaxial tensile strain loading. Figure 5 shows the simulated ultimate strength of ultrathin Ni nanowires as a function of nanowire length for different temperatures. As expected, the nanowire strength decreases with increase of temperature for all the given nanowire length. It is believed that the temperature softening results from the weaker bonds between Ni atoms caused by the increasing temperature. By comparing the results in Fig. 5, it is found that for all the temperatures and nanowire lengths', the strength becomes lower as nanowire length increases. Figure 5 shows decreases in strength with increasing nanowire length at different temperatures.

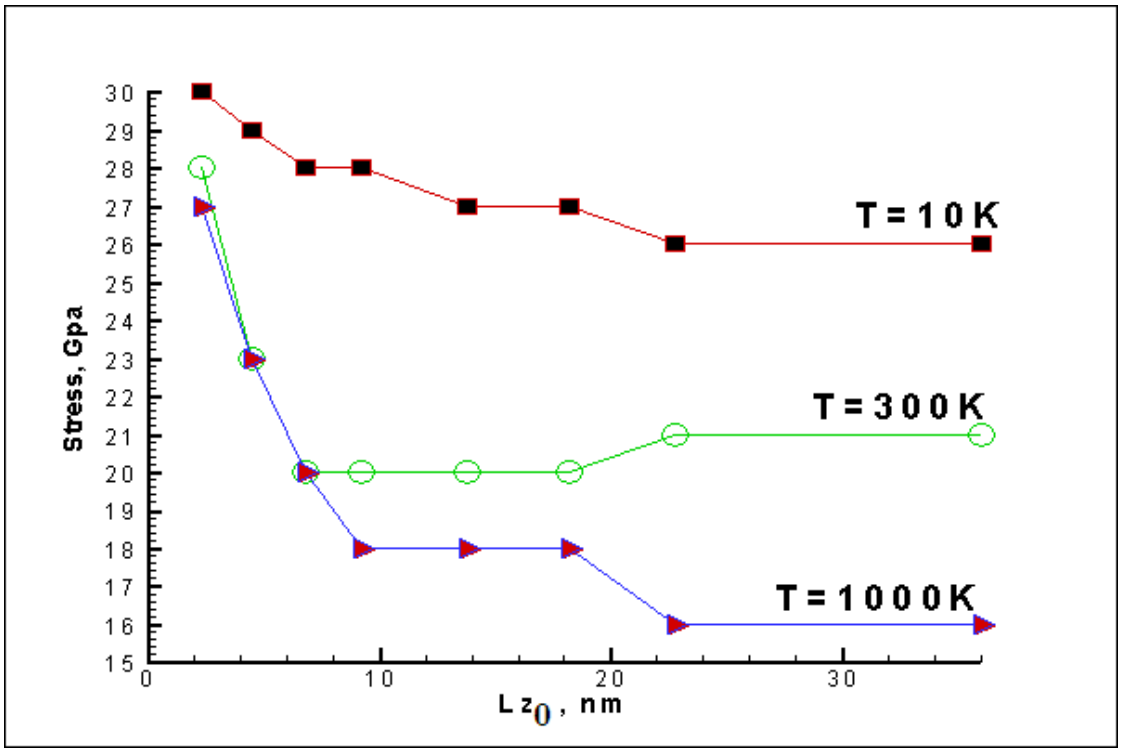

Fig. 5. The simulated ultimate strength of ultrathin Ni nanowires as a function of nanowire length for different temperatures.

5. Breaking position

The results showed that the breaking position depended on the nanowire length (Fig. 6). When it was less than 6.8 nm, the most probable breaking position was located at the center of the nanowires. However, it gradually shifted to the ends as the nanowire length increased over 6.8 nm as in Tables 1, 2 and 3. Figure 6 presents the calculated breaking position for ultrathin Ni nanowires as a function of nanowire length for different temperatures. Unlike the strength, the calculated breaking position increases with increasing temperature. This result implies that the temperature and nanowire length may have a strong effect on the breaking position. It is worth noting, as shown in Figs. 5 and 6, that the long dependence of the breaking position is completely difference from that of the strength. Figure 7 is a snapshot of the atomic breaking of Ni of different lengths. As can be seen from the figure and the results shown in Table 2 with the length of the sample breaking occurs at higher strains. Status of breaking depends on the length of the samples.

Table 1. MD calculation results of different system at 10 K, depending on the number of atoms (N), the initial length (l_0), yield strength (σ_T), the start of plastic deformation (t_{pl}), yielding length (l_{z1}), yielding strain (ε), breaking time (t_d), breaking length (l_b) and breaking position (P_b).

	System	N	l_0, nm	σ, GPa	t_{pl}, ps	l_{z1}, nm	Ɛ, %	t_d	l_b, nm	P_b
1	5x5x5	63	2.3	30	9	2.6	0.13	45	4.1	2
2	5x5x10	125	4.5	29	17	5.4	0.2	85	9	4.5
3	5x5x15	188	6.8	28	25	8.1	0.19	58	9.8	5.5
4	5x5x20	250	9.2	28	33	10.8	0.17	84	13.1	5.5
5	5x5x30	375	13.8	27	48	16.2	0.173	91	18.5	10.2
6	5x5x40	500	18.2	27	64	21.5	0.18	119	26.3	11.5
7	5x5x50	625	22.8	26	80	27	0.184	91	35.8	13.5
8	5x5x90	1125	36	26	140	41	0.138	148	48	8

Table 2. MD calculation results of different system at 300 K, depending on the number of atoms (N), the initial length (l_0), yield strength (σ_T), the start of plastic deformation (t_{pl}), yielding length (l_{z1}), yielding strain (ε), breaking time (t_d), breaking length (l_b) and breaking position (P_b).

	System	N	l_0, nm	σ, GPa	t_{pl}, ps	l_{z1}, nm	Ɛ, %	t_d	l_b, nm	P_b
1	5x5x5	63	2.3	28	9	2.4	0.043	66	5.8	2.6
2	5x5x10	125	4.5	23	15	5.3	0.17	55	7.4	4
3	5x5x15	188	6.8	20	19	7.8	0.147	56	10	4.5
4	5x5x20	250	9.2	20	24	10.5	0.141	75	13.2	6.5
5	5x5x30	375	13.8	20	42	16	0.084	70	17.5	8.8
6	5x5x40	500	18.2	20	52	22	0.208	75	22.4	13
7	5x5x50	625	22.8	21	60	26	0.14	102	28.2	16
8	5x5x100	1250	44.8	21	120	52.2	0.165	125	52	26
9	5x5x150	1875	67.2	21	165	76	0.13	190	78	30

Table 3. MD calculation results of different system at 1000 K, depending on the number of atoms (N), the initial length (l_0), yield strength (σ_T), the start of plastic deformation (t_{pl}), yielding length (l_{z1}), yielding strain (ε), breaking time (t_d), breaking length (l_b) and breaking position (P_b).

	System	N	l_0, nm	σ, GPa	t_{pl}, ps	l_{z1}, nm	Ɛ, %	t_d	l_b, nm	P_b
1	5x5x5	63	2.3	27	9	2.4	0.043	54	5.2	2.5
2	5x5x10	125	4.5	23	15	5.1	0.133	66	8.2	3.2
3	5x5x15	188	6.4	20	20	7.5	0171	60	10.3	5.5
4	5x5x20	250	9.2	18	25	9.8	0.065	62	12.6	6.1
5	5x5x30	375	13.8	18	39	14.7	0.065	58	17.3	8.2
6	5x5x40	500	18.2	18	51	19.2	0.055	47	21.5	9
7	5x5x50	625	22.8	16	58	23.8	0.044	35	25.2	13.5
8	5x5x95	1188	44.4	16	115	45.6	0.027	30	46.8	23.2

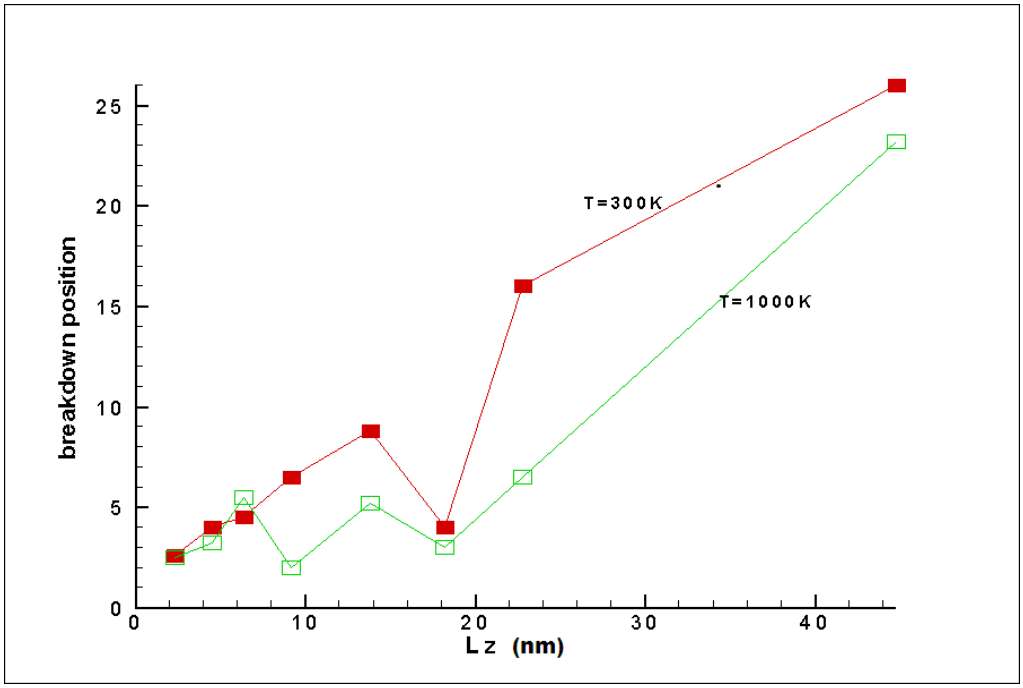

Fig. 6. The calculated breaking position for ultrathin Ni nanowires as a function of nanowire length for different temperatures.

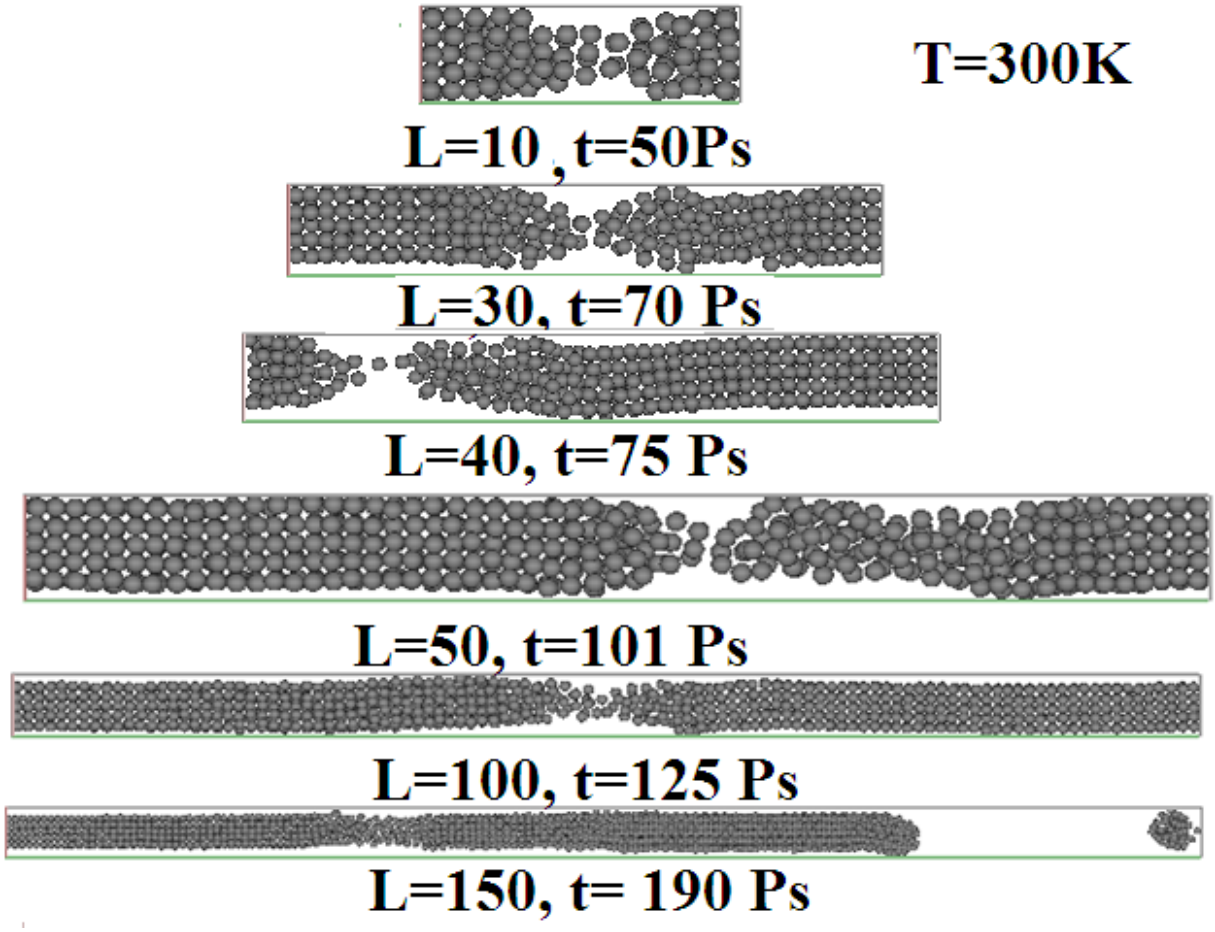

Fig. 7. Atomic structure of Ni nanowires of different lengths at the time of breaking of the crystal.

6. Conclusion

1. As a result of structural studies of energy transformation in the process of deformation and fracture of fcc Ni, with different length of the uniaxial tensile strain at various temperatures produced four stages of features structurally energy transformations: quasielastic , plastic , flow and failure (Fig. 4a).
2. The length of nanowire influences the magnitude of the time interval between the beginning of the elastic deformation and plastic deformation phase duration. By increasing the length of the specimen, the yield stress decreases and the duration of a quasi-elastic deformation increases. With increasing temperature, the values of these parameters are reduced.
3. Regulation of failure depends on the length of nanowire. Apparently for small samples is an important influence of the surface atoms, the proportion decreases with increasing sample size. Surface atoms play an important role in the mechanical behavior of nanostructures. Although individual case of destruction is not predictable, many cases of failure show statistics behavior. In most cases, with a relatively small size nanowire, the final position of fracture occurs in the central part, as the length of nanowire increases, the position of breaking position is gradually shifted towards the ends. The simulation results would be helpful to avoid the materials failure by predicting the breaking position. Several snapshots of the system revealed this ductile character, including the necking of the nanowire before failure.

References

[1] M.D. Starostenkov, M.M. Aish, A.A. Sitnikov, S. A. Kotrechko // *Letters on Materials* **3** (2013) 180.
[2] Wei-dong Wang, Cheng-long Yi, Kang-qi Fan // *Transactions of Nonferrous Metals Society of China* **23(11)** (2013) 3353.
[3] Zhou Zhao-feng, Pan Yong, Lei Wei-xin // *Transactions of Nonferrous Metals Society of China* **20(4)** (2010) 637.
[4] Cheng Peng, Yuan Zhong, Yang Lu, Sankar Narayanan, Ting Zhu, Jun Lou // *Applied Physics Letters* **102(8)** (2013) 083102.
[5] Yu-Hua Wen, Zi-Zhong Zhu, Ru-Zeng Zhu // *Computational Materials Science* **41** (2008) 553.
[6] M.M. Aish, M.D. Starostenkov // *Materials Physics and Mechanics* **18(1)** (2013) 53.
[7] H. Rafii-Tabar // *Physics Reports* **325(6)** (2000) 239.
[8] E.V. Kozlov, L.E. Popov, M.D. Starostenkov // *Russian Physics Journal* **15(3)** (1972) 395.
[9] L.A. Girifalco, V.G. Weizer // *Physical Review* **114** (1959) 687.
[10] S.V. Dmitriev, A.A. Ovcharov, M.D. Starostenkov, E.V. Kozlov // *Physics of the Solid State* **38(6)** (1996) 996.
[11] X. Yang, L. Liu, P. Zhai, Q. Zhang // *Computational Materials Science* **44** (2009) 1390.
[12] A.I. Potekaev, E.A. Dudnik, L.A. Popova, M.D. Starostenkov // *Russian Physics Journal* **51(10)** (2008) 1053.
[13] M.D. Starostenkov, B.F. Demyanov, S.L. Kustov, E.G. Sverdlova, E.L. Grakhov // *Computational Materials Science* **14** (1999) 146.